Link Power Optimization for S+C+L Multi-band WDM Coherent Transmission Systems

Salma Escobar Landero, Ivan Fernandez de Jauregui Ruiz, Alessio Ferrari, Dylan Le Gac, Yann Frignac, Gabriel Charlet
Huawei Technologies France, Paris Research Center, Optical Communication Technology Lab
salma.escobar.landero@huawei.com

Abstract: We compare S+C+L link power optimization based on the fast and simple heuristic balance of linear and nonlinear noises versus more complex ML-based techniques to estimate optimum per-band line amplifier settings for system capacity maximization.

1. Introduction

Expanding per-fiber available transmission bandwidth is a straightforward solution to increase the capacity of current WDM optical fiber networks. Multi-band S+C+L systems up to 16 THz using discrete-only amplification have been experimentally demonstrated [1-2]. In these ultra-wide multi-band systems, performance is severely affected by the nonlinear inter-channel stimulated Raman scattering (ISRS) effect. Power optimization techniques are therefore required to proper balance power transfer between bands, thus maximizing system capacity [1-6].

In the absence of ISRS, it is well known from the Gaussian Noise (GN) model that at the optimum channel power, amplified spontaneous emission (ASE) noise power is twice the Kerr-nonlinear (NL) noise power ($P_{ASE}/P_{NL} = 2$) [7]. This property makes power optimization very simple as optimal power can be derived analytically. However, in the presence of ISRS, power optimization is a non-convex problem leading to multiple local solutions. For this purpose, the use of machine learning (ML) evolutionary algorithms such as the *genetic-algorithm* (GA) and the *particle swarm optimization* (PSO) algorithm have been investigated [2-4]. Exhaustive search has also been addressed [6], while a first attempt to generalize the P_{ASE}/P_{NL} rule has been shown in [8]. In this work we compare S+C+L power optimization based on an iterative version of the simple heuristic P_{ASE}/P_{NL} technique (ASENL hereafter) and the more powerful but complex GA- and PSO-based approaches. We show that the first allows near optimum power optimization with lower required complexity, making it suitable for fast system design and re-optimization tools.

2. OMS definition and SNR estimation model

Fig.1(a) shows the basic structure of the considered S+C+L optical multiplexing section (OMS). At the input/output, wavelength selective switches (WSS) are used for channel add-drop capabilities as well as for per-channel power equalization. Individual per-band amplifiers are employed to compensate for span loss and to adjust launched power into the fiber. SCL multiplexers/demultiplexers with 1dB insertion loss each are used at each amplification stage.

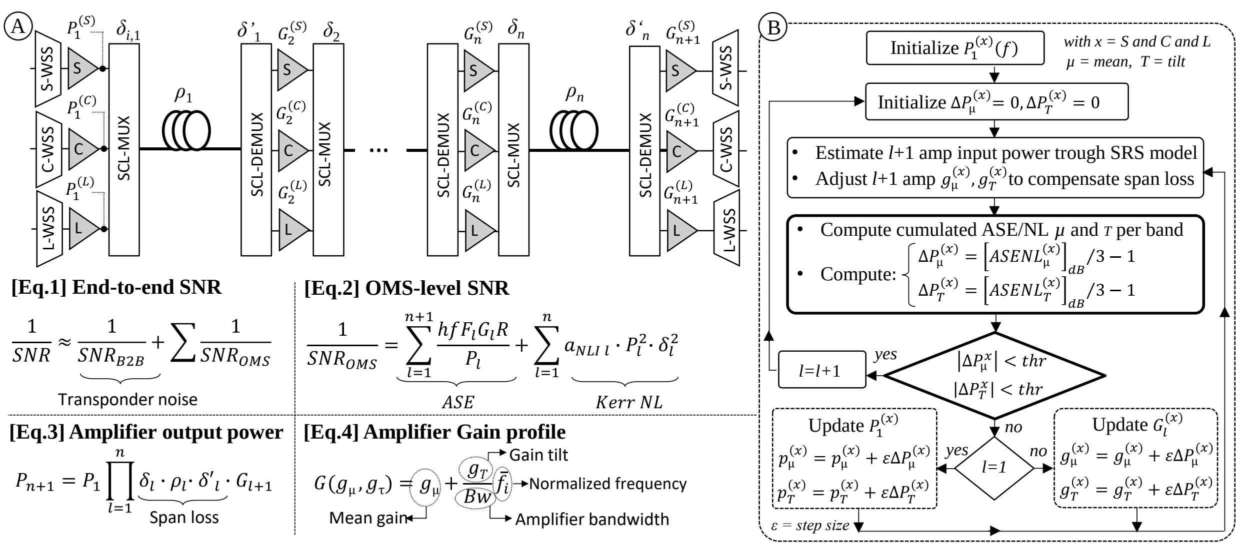

Fig.1. (a) S+C+L OMS section composed of wavelength selective switches (WSS), optical amplifiers, SCL multiplexer/demultiplexers, and fiber spans. (b) Block diagram of OMS-based amplifier gain/power optimization based on heuristic P_{ASE}/P_{NL} ratio.

The end-to-end SNR performance of any WDM channel over a given optical link composed of k OMS can be obtained following Eq. 1 (inset Fig. 1). The SNR_{OMS} (Eq. 2) corresponds to the SNR of each OMS arising from the independent contributions of ASE and NL noises at each l'th span inside the OMS. Each amplifier is characterized by its noise figure (F), its gain (G), and output power (P) frequency profiles. h is Planck's constant and f is frequency. Each span is characterized by its input/output SCL multiplexer/demultiplexers with intrinsic lumped losses δ and δ' respectively, by its fiber nonlinear coefficient (a_{NLI}) accounting for fiber Kerr-effects, and by its fiber frequency dependent loss (ρ); the two-last accounting for ISRS effect. The transponder back-to-back SNR (SNR_{B2B}) can be obtained experimentally [9]. Power evolution along the OMS can be estimated using Eq. 3. The term a_{NLI} is computed as per [10]. Fiber attenuation and Raman parameter fitting within a_{NLI} is *mandatory* to account for bandwidths above 15 THz and tilted fiber input power profiles [10]. ρ is computed based on Raman ordinary differential equations (ODE) using experimentally measured Raman gain. Optical in-line filtering is left out of the scope of this work as optimum power is independent on filtering [11]. The system is assumed to be fully loaded.

3. OMS-based power optimization method description

Dynamic per-channel equalization is assumed to be possible only at the OMS input WSS, with all in-line amplifiers having *static* (for a given load/gain) gain profiles. For practical system design purposes and without loss of generality, we consider ideal flat-tilted amplifier gain profiles defined by their nominal mean gains (g_μ) and tilts (g_T) as Eq. 4. Real measured gain profiles for different g_μ, g_T could eventually be used. Booster output power profile is also considered to be flat-tilted defined by its mean power ($P_{1\mu}$) and tilt (P_{1T}) for each band. The power optimization process consists on finding the optimum per-band booster $P_{1\mu}$, and P_{1T} as well as the per-band in-line amplifiers g_μ, g_T to maximize capacity. The optimum power/gain mean and tilts can serve for simple OMS design strategies while dynamic per-channel equalization at WSS level can be applied for real in-field power ripples.

We investigate power optimization based on a GA, a PSO, and the simple heuristic ASENL method. For this last case, due to the presence of ISRS, single-step optimum power computation is not possible. Therefore, we perform an iterative approach depicted in Fig.1(b) and described as follows: For the first span within the OMS (l=1), booster output power $P_1(f)$ for each band (x) is initialized to any flat power profile. Input power to the next amplification stage (l+1) is computed from δ, δ', and ρ terms. l+1 amplifiers g_μ and g_T are set to compensate for per-band span loss. Mean and tilt of the frequency dependent P_{ASE}/P_{NL} ratio for each band is computed, from which the power distance to optimum is derived ($\Delta P = (P_{ASE}/P_{NL})_{dB}/3 - 1$). Booster mean output power and tilt are updated based on a fraction (ε) of ΔP. The operation is repeated until ΔP is below a given desired threshold. This process is repeated sequentially for all consecutive spans. However, it is the mean gains and tilts of all inline amplifiers which are optimized, for which the output power is computed based on Eq. 3 accounting for the entire power evolution from l=1 to l= n. Similarly, cumulated P_{ASE}/P_{NL} is computed for each new optimized span. This process allows to account for heterogeneous spans and cumulated power variations due to frequency dependent fiber attenuation coefficient, ISRS gain, and eventually amplifier gain ripples. For GA- and PSO-based optimizations, we follow a similar sequential cumulated span-by-span process where $P_{1\mu}$, P_{1T}, g_μ, g_T are updated such that the total Shannon capacity is maximized (i.e. $\sum 2\log_2(1 + SNR_i)$) [6]. For PSO, a subsequent gradient descent (GD) is used for final convergence.

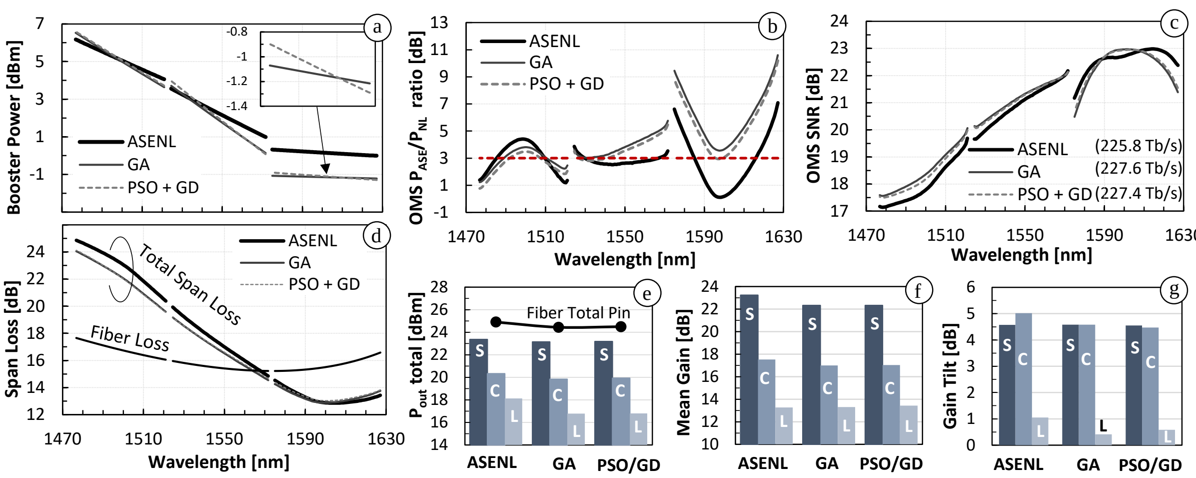

Fig.2. (a) Booster output power, (b) P_{ASE}/P_{NL} ratio, (c) OMS SNR, (d) Span Loss. Optimum amplifier (e) total output power, (f) mean gains, and (g) gain tilt for all studied power optimization techniques.

4. Power Optimization Simulation Results

We first consider a single OMS composed of 5x80km SMF fiber spans. 184x600 Gb/s PCS64QAM channels are distributed over S, C and L bands with 100 GHz spacing for a total of 18.4 THz bandwidth. Noise figure of all amplifiers is considered to be 4.5dB for simpler results comparison. Fig.2(a) shows the optimized booster output power for each of the studied algorithms. Both GA- and PSO-based approaches converge to similar solutions, leading to non-flat power profiles with S-band requiring ~6.5dB (~3dB) higher output power compared to L-band (C-band). The ASENL technique leads to ~0.3/0.4/1.3dB higher launched power for S/C/L bands compared to GA and PSO. Fig.2(b) shows the total OMS P_{ASE}/P_{NL} ratio for the three methods. As expected, the mean ratio converges to 3dB for the ASENL, while for GA and PSO both C- and L-bands are slightly pushed to the “linear” regime. The total OMS SNR is shown in Fig.2(c), showing that both GA and PSO achieve a slightly higher SNR compared to the ASENL for both S- and C-band (~0.3dB), while it is globally decreased for L-band with up to ~1dB degradation for higher wavelengths. Both GA- and PSO-based approaches increase performance in S- and C-bands at the cost of L-band degradation to maximize global capacity. A ~6dB SNR tilt is observed over the entire spectrum. The curved-shape of L-band is due to the accumulation of fiber frequency dependent attenuation and ISRS gain. Fig.2(d) shows the corresponding span loss for the three techniques. Compared to the heuristic ASENL, both GA and PSO achieve a lower span loss (therefore higher performance) in both S- and C-bands while it is mainly unchanged for the L-band. The total achieved OMS Shannon capacities are 225.8/227.6/227.4 Tb/s for ASENL/GA/PSO approaches respectively. The simple and fast heuristic ASENL approach leads to a loss of 0.7% in total capacity requiring ~10% higher launched power into the fiber. Fig.2 (e) shows the total output power per band, Fig.2 (f) and (g) show the mean amplifier gains and tilts for all studied techniques. It is clear the big unbalance of the required amplifier output powers and gains between the three bands. Fig. 3(a) shows the amplifier output power profile along the OMS.

Once optimum OMS amplifier settings have been obtained, a per-channel equalization can be performed at WSS level to account for power ripples accumulation. In this sense, booster-only per-channel output power profile is optimized based on the heuristic ASENL approach similar to [11], under the constraint that total output power per-band should be maintained to avoid important changes in ISRS power transfer. Fig. 3(b) shows the new equalized amplifier output power profile along the OMS, while Fig. 3(c) shows the corresponding OMS SNR. Performance is improved for all channels (1dB max) leading to a total Shannon capacity increase from 225.8 Tb/s to 226.6 Tb/s.

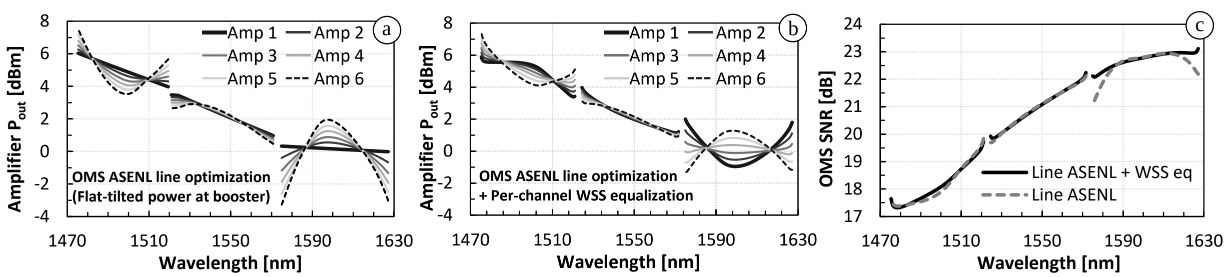

Fig.3. Amplifier output power profile for ASENL-based line-optimization for (a) flat-tilted booster profile and (b) per-channel WSS equalization. (C) OMS SNR with and without per-channel WSS equalization at OMS input.

5. Conclusions

Multi-band S+C+L link power optimization using evolutionary ML-based GA and PSO algorithms have been compared to an iterative version of the simplest and fastest heuristic ASENL method based on the balance of linear and nonlinear noises. ASENL achieves near optimum results with only ~0.7% capacity decrease, making it suitable for fast design or reconfiguration strategies in future multi-band systems highly impacted by ISRS effect.

6. References

[1] F. Hamaoka et al., "Ultra-Wideband WDM Transmission in S-, C-, and L-Bands Using Signal Power Optimization Scheme," JLT (2019)
[2] H. Buglia et al., "Challenges in Extending Optical Fibre Transmission Bandwidth Beyond C+L Band and How to Get There," ONDM, (2021)
[3] D. Semrau et al., "Modeling and mitigation of fiber nonlinearity in wideband optical signal transmission," JOCN (2020)
[4] N. A. Shevchenko et al., "Ultra-Wideband Information Throughput Attained via Launch Power Allocation," ONDM (2021)
[5] I. Roberts et al., “Channel power optimization of WDM systems following Gaussian noise nonlinearity model in presence of stimulated Raman scattering,” JLT (2017).
[6] A. Souza et al., “Optimized Deployment of S-band and Raman Amplification to Cost-Effectively Upgrade Wideband Optical Networks,” ECOC (2021)
[7] P. Poggiolini et al., "The LOGON strategy for low-complexity control plane implementation in new-generation flexible networks," OFC (2013)
[8] V. V. Garbhapu et al.,” Network-Wide SNR-based Channel Power Optimization,” ECOC (2021)
[9] T. Zami, et al., “Simple self-optimization of WDM networks based on probabilistic constellation shaping," JOCN (2020)
[10] D. Semrau et al., “A modulation format correction formula for the Gaussian noise model in the presence of inter-channel stimulated Raman scattering,” JLT (2019)
[11] I. F. de Jauregui Ruiz et al., “An accurate model for system performance analysis of optical fiber networks with in-line filtering,” ECOC (2019)